CONF-870413--17

ANL-HEP-CP-87-82
For the Proceedings of the
XI International Conference
on Particles and Nuclei
Kyoto, Japan April, 1987

NN ELASTIC SCATTERING EXPERIMENTS WITH POLARIZED BEAMS

T. Shima

Argonne National Laboratory, Argonne, IL 60439 USA

ANL-HEP-CP--87-82

DE88 003108

ABSTRACT

We report updated analysis results on an np elastic experiment at LAMPF and a pp experiment at the ZGS. We have measured two np spin asymmetry parameters, C_{LL} and C_{SL}, at beam energies 500, 650, and 800 MeV. The cm scattering angles of neutrons measured ranged from 80° through 180°. We observed very large C_{LL} at backward angles for the first time[1]. The pp experiment at the ZGS was a measurement of the difference between the pp total cross sections for parallel and antiparallel longitudinal spin states at beam momenta 2.75, 2.92, 3.25, 3.75, and 4.00 GeV/c. These results reveal possible new structures in this momentum range. Masses for these structures are about 2700 and 2900 MeV[2].

INTRODUCTION

Our main interests in continuing nucleon-nucleon experiments at LAMPF after completing the ZGS experiments rely on the following facts:

i) We have observed structure in the pp elastic channel (pure I = 1) and in the np elastic channel (I = 1 and I = 0) at the ZGS, and therefore we were motivated to further study these structures[3].

ii) Good quality np experimental data with polarized beam and/or target at intermediate energy are very sparse compared with the pp data base[4]. The np data are indispensable for the phase shift analysis (PSA) and the determination of spin dependent amplitudes. We have

DISCLAIMER

completed the first phase of the np experiments and are working on the second phase of the np experiments at LAMPF.

We define the amplitudes and observables as:

i) s-channel helicity amplitudes

$$\langle ++|++\rangle = \phi_1$$

$$\langle ++|--\rangle = \phi_2$$

$$\langle +-|+-\rangle = \phi_3$$

$$\langle +-|-+\rangle = \phi_4$$

$$\langle ++|+-\rangle = \phi_5$$

and

ii) laboratory observables

$\sigma^{Tot} = (0,0;0,0)$	$(2\pi/k)\ \mathrm{Im}\{\phi_1(0) + \phi_3(0)\} = 1/2\ \{\sigma(\downarrow\uparrow) + \sigma(\uparrow\uparrow)\}$
	$= 1/2\ \{\sigma(\rightleftarrows) + \sigma(\rightrightarrows)\}$
$\Delta\sigma_T = (N,N;0,0)$	$-(4\pi/k)\ \mathrm{Im}\ \{\phi_2(0)\} = \sigma(\uparrow\downarrow) - \sigma(\uparrow\uparrow)$
$\Delta\sigma_L = (L,L;0,0)$	$(4\pi/k)\ \mathrm{Im}\ \{\phi_1(0) - \phi_3\ (0)\} = \sigma\ (\rightleftarrows) - \sigma\ (\rightrightarrows)$
$\sigma = (0,0;0,0)$	$1/2(\lvert\phi_1\rvert^2 + \lvert\phi_2\rvert^2 + \lvert\phi_3\rvert^2 + \lvert\phi_4\rvert^2 + 4\lvert\phi_5\rvert^2)$
$P = (0,N;0,0)$	$\mathrm{Im}\ \{(\phi_1 + \phi_2 + \phi_3 - \phi_4)^*\phi_5\}/\sigma$
$C_{LL} = (L,L;0,0)$	$-1/2(\lvert\phi_1\rvert^2 + \lvert\phi_2\rvert^2 - \lvert\phi_3\rvert^2 - \lvert\phi_4\rvert^2)/\sigma$
$C_{SL} = (S,L;0,0)$	$\mathrm{Re}\ \{(\phi_1 + \phi_2 - \phi_3 + \phi_4)^*\ \phi_5\}/\sigma$
$C_{SS} = (S,S;0,0)$	$\mathrm{Re}(\phi_1^*\phi_2 + \phi_3^*\phi_4)/\sigma$
$C_{NN} = (N,N;0,0)$	$(\mathrm{Re}\{(\phi_1^*\phi_2 - \phi_3^*\phi_4) + 2\ \lvert\phi_5\rvert^2\}/\sigma$

The past extensive ZGS polarization data on the pp elastic scattering at 6 GeV/c made possible determinations of the pp amplitudes in the different channels, helicity and exchange[5]. It was found at small angles that the spin nonflip amplitudes, ϕ_1 and ϕ_3, are much larger than spin flip amplitudes, ϕ_2, ϕ_4 and ϕ_5. Furthermore, helicity conservation requires ϕ_4 and ϕ_5 amplitudes to vanish at 0°[5].

The np Experiment at LAMPF

The spin asymmetry measurements were performed using high energy polarized neutron beams produced via charge exchange in the reaction pd → npp at 0°. The spin of the neutron beam was precessed to either along the beam direction or perpendicular to the beam direction in the scattering plane[7]. The neutron beam then scattered in a polarized proton target. The protons in the target were dynamically polarized by microwaves and were kept at a temperature of 0.5 K. More than 85% of the target consisted of carbon and oxygen atoms.

In our data analysis we reconstruct trajectories of events using coordinate information from the chambers and then we calculated the momenta. The elastic events were accumulated in four different missing mass histograms depending on the beam and the target spin directions.

The results of the measurements are shown in Fig. 2 along with phase shift predictions. The C_{LL}'s at 500 and 650 MeV are very small up to about 90° and then start rising very rapidly. At 180° the C_{LL}'s drop to become almost -1. One possible explanation of the C_{LL} behavior around 180° is to assume ϕ_3 is much larger than the other amplitudes around 120°. Then the large positive C_{LL} value around 120° is caused by ϕ_3 from the C_{LL} formula quoted earlier. From the symmetry relationships among the helicity amplitudes[6],

$$\phi_3(180^\circ - \theta) = (-1)^{I} \phi_4(\theta)$$

where I = isospin. Since $\phi_4 = 0$ at 0°, then ϕ_3 (180°) = 0. Therefore, the drop in C_{LL} as $\theta \rightarrow 180°$ is caused by the vanishing of ϕ_3. Furthermore, since the measured C_{LL} value at 180° is nearly -1.0, we expect $(|\phi_1|^2 + |\phi_2|^2) \gg |\phi_4|^2$. This means that ϕ_4 is also small at 180° but need not be small around 120°. Therefore, there are two large amplitudes at 180°, both with parallel initial spin states. The measured C_{SL}'s at 500 and 650 MeV are less than about 35% in magnitude and they may not be as small as some PSA's predict. We observe that C_{SL} is zero at 0° because of ϕ_5, which vanishes at 0° and the C_{SL} formula quoted earlier. We are now analyzing the 800 MeV data.

New Results on $\Delta\sigma_L$ from the ZGS

We performed, in the past, a series of pp scattering experiments at beam momenta from 1.2 thru 11.75 GeV/c at the ZGS. A history of ZGS experiments is summarized by A. Yokosawa[8]. We will be discussing here new results on measurements of the difference of the pp total cross sections for parallel and antiparallel longitudinal spin states at beam momenta 2.75, 2.92 3.25, 3.48, 3.75, and 4.00 GeV/c[9]. Our results on the previous measurements of the $\Delta\sigma_L$ up to 6.00 GeV/c are reported in Refs. 10 and 11. The data of Ref. 10 are shown in Fig. 1. The dip and peak structures have been interpreted as evidence for the formation of diproton resonances $B^2(2.14)$ with a quantum state of $^1D_2$, and $B^2(2.22)$ with $^3F_3$ state[12]. We attempted to look for additional $\Delta\sigma_L$ structure in the momentum region higher than those previously found. The experiment was similar to that previously reported[10]. The results obtained are shown in Fig. 3 along with some of the previous data[10]. To study the behavior of the partial scattering amplitudes, the data on the dimensionless quantity $(k^2/4\pi)\Delta\sigma_L$ are plotted in Fig. 4 as a function of the center-of-mass energy, where k is c.m. momentum. If the bumps in $(k^2/4\pi)\Delta\sigma_L$ are considered to be due to resonances, the masses are about 2700 and 2900 MeV. We note here that indications of these structures were first reported in different measurements[13,14]. Assignments of the quantum states for both resonances have not been confirmed, but they are spin singlets since they both appear as bumps in the $\Delta\sigma_L$ plots.

Concluding Remarks

It is difficult to find out whether the observed resonances in the $I = 1$ channel are due to the formation of dibaryons, from both the experimental and theoretical points of view. Experimentally, it is difficult to isolate a dibaryon from NN, NΔ,and ΔΔ unless one observes a large resonance with a very narrow width since one may expect a dibaryon to be a well defined state. Dibaryon resonances are discussed in the MIT bag model[15] and the quark cluster model[16]. Interestingly enough, some predictions on mass spectra for $I = 0$ from both the bag model and the quark cluster model produce the same lowest mass around 2160 MeV[17]. This mass corresponds to a beam kinetic energy of around 610 MeV where we measured the spin asymmetries at LAMPF.

---

§ Work supported by the U.S. Department of Energy, Division of High Energy Physics, Contract W-31-109-ENG-38.

References

[1] Participants on this experiment are:

W. R. Ditzler, D. Hill, J. Hoftiezer, K. Johnson, D. Lopiano, T. Shima, H. Shimizu, H. Spinka, R. Stanek, D. Underwood, R. Wagner and A. Yokosawa Argonne National Laboratory, Argonne, IL 60439 USA.

T. S. Bhatia, G. Glass, J. C. Hiebert, R. A. Kenefick, S. Nath and L. C. Northcliffe Texas A&M University, College Station, TX 77843 USA.

R. Damjanovich, and J. J. Jarmer, Los Alamos National Laboratory, Los Alamos, NM 87544 USA.

G. Burleson, J. Faucett, C. Fontenla, R. Garnett and M. Rawool New Mexico State University, Las Cruces, NM 88003 USA.

R. H. Jeppesen University of Montana, Missoula, MT 50812 USA.

G. E. Tripard Washinghton State University, Pullman, WA 99164 USA

[2] Participants on this experiment are:

I. P. Auer, E. Colton, H. Halpern, D. Hill, R. C. Miller, H. Spinka, G. Theodosiou, K. Toshioka, D. Underwood, R. Wagner, and A. Yokosawa Argonne National Laboratory, Argonne, IL 60430 USA

[3] For I=1 ZGS experiments:

(a) I. P. Auer et al., Phys. Lett. 67B (1977) 113;

(b) ibid. 70B (1977) 475;

(c) Phys. Rev. Lett. 41 (1978) 354.

For I = 0 ZGS experiment; Phys. Rev. Lett. 46 (1981) 1177, also see Fig. 1.

[4] For example, see R. A. Arndt et al., Phys. Rev. D35 (1987) 128.

[5] For the amplitude determination, see I. P. Auer et al. Phys. Rev. D32 (1985) 1609. Detailed discussion on helicity amplitudes is found, for example, in M. L. Goldberger et al., Phys. Rev. 120 (1960) 2250. Helicity amplitudes may be decomposed in terms of partial waves, which

we use as a tool to investigate structures in cross sections. For example, see, for a starting place, A. Yokosawa, Phys. Reports, 64, No2 (1980) 47-86.

[6] See the papers by M. L. Goldberger et al. in Ref. 5, and H. Spinka, Phys. Rev. D30 (1984) 1461. The latter paper has experimentally useful expressions relating I = 1 and I = 0.

[7] The experimental setup for this experiment is found in J. S. Chalmers et al., Proc. Sixth Int. Symp. Polar. Phenom. in Nucl. Phys., Osaka, 1985 (J. Phys. Soc. Jap. 55 (1986) Suppl. P910-911).

[8] See the second reference in [5]

[9] Results from 2.75 to 3.48 GeV/c were published in I. P. Auer et al., Phys. Rev. D34 (1986) 2581.

[10] Same as in ref. 3 for I=1.

[11] LAMPF experiment at beam kinetic energy from 300 thru 800 MeV; I. P. Auer et al., Phys. Rev. D29 (1984) 2435.

[12] For latest summary, see A. Yokosawa, Proc. Sixth Int. Symp. Polar. Phenom. in Nucl. Phys., Osaka, Japan, 1985 (J. Phys. Soc. Jpn., 55 (1986) Suppl. P251-271)

[13] See Ref. 12

[14] I. P. Auer et al., Phys. Rev. Lett., 48 (1982) 1150.

[15] For example, see A. Th. M. Aerts et al., Phys. Rev. D17 (1978) 260 P. J. G. Mulder et al., Phys. Rev. Lett., 40, (1978) 1543 and E. L. Lomon, Nuclear Physics, A434, (1985) 139c.

[16] For example, see D. B. Lichtenberg et al., Phys. Rev. D18 (1978) 2560; and N. Konno et al. Phys. Rev., D35 (1987) 239.

[17] See the papers by Mulder et al. Ref. 15, and N. Konno et al., Ref. 16.

FIGURE CAPTIONS

Figure 1 $\Delta\sigma_L$ vs. P_{lab} in pure $I=0$ and $I=1$ channel. The lines drawn are to guide the eyes.

Figure 2 C_{LL} and C_{SL} vs. θ at beam kinetic energies 500, 650, and 800 MeV. The lines drawn are phase shift predictions. The dark circles with the error bars are measured values. The errors include the systematic errors estimated at this time.

Figure 3 A plot of $\Delta\sigma_L$ vs. P_{lab} in pp scattering. The circles with error bars are measured values. The line drawn is to guide the eyes.

Figure 4 A plot of $(k^2/4\pi)\Delta\sigma_L$ vs. P_{lab}. The same quantity as in Fig. 3 except a factor of $k^2/4\pi$.

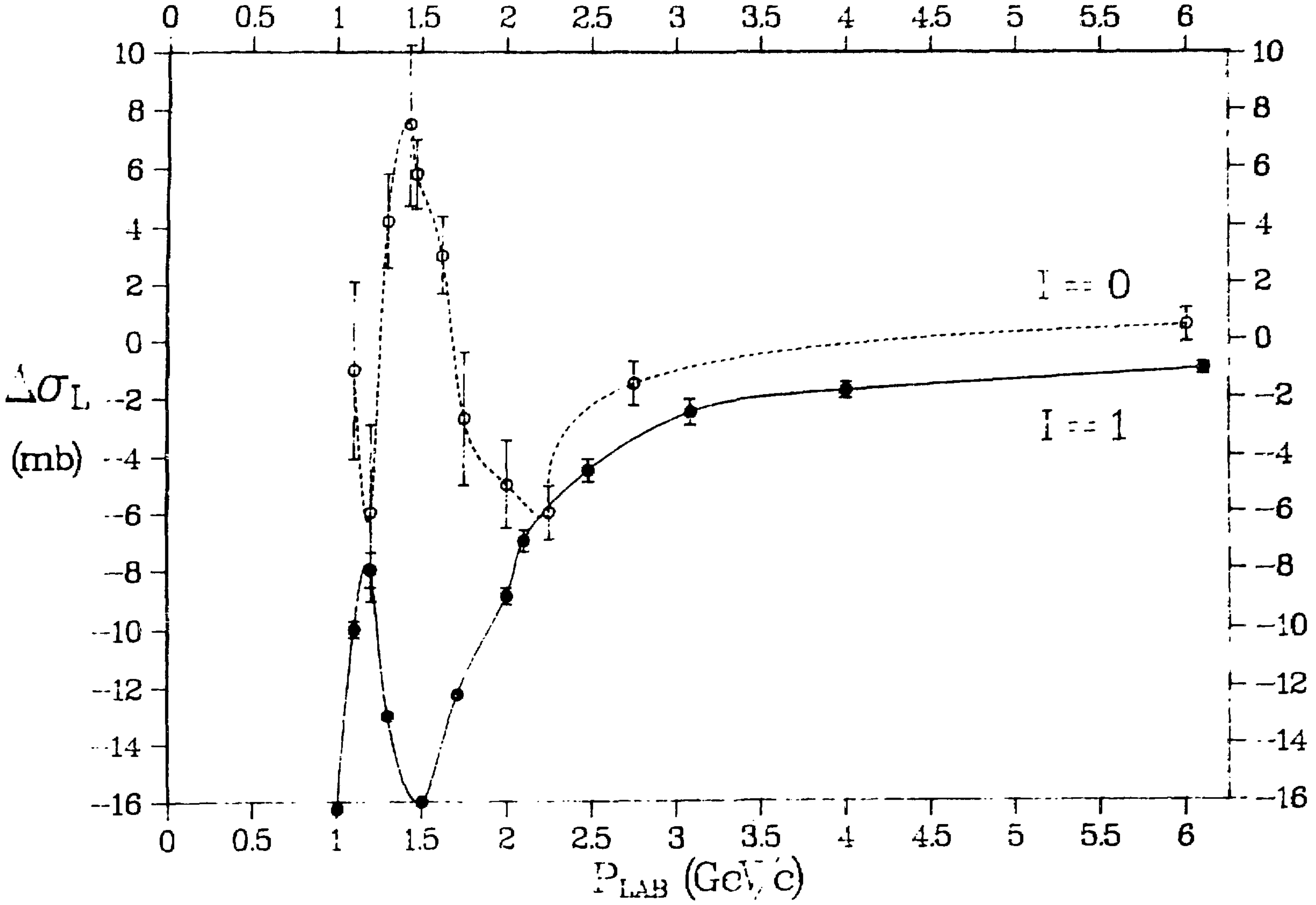
$\Delta\sigma_L$ (mb)
10
8
6
4
2
0
-2
-4
-6
-8
-10
-12
-14
-16
0
0.5
1
1.5
2
2.5
3
3.5
4
4.5
5
5.5
6
I = 0
I = 1
p_{LAB} (GeV/c)

Figure 1

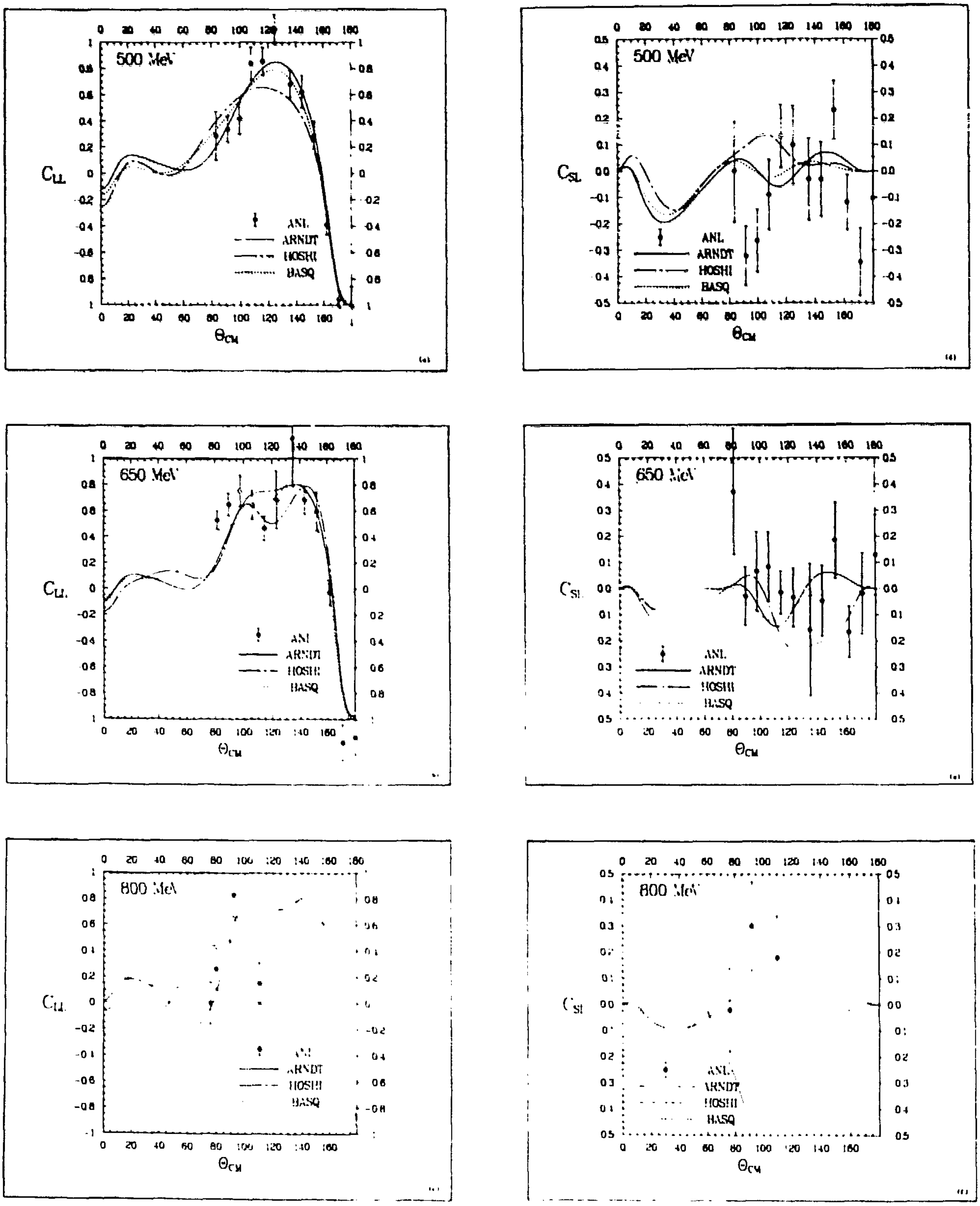
500 MeV
C_LL
Θ_CM
ANL
ARNDT
HOSHI
BASQ
500 MeV
C_SL
Θ_CM
ANL
ARNDT
HOSHI
BASQ
650 MeV
C_LL
Θ_CM
ANL
ARNDT
HOSHI
BASQ
650 MeV
C_SL
Θ_CM
ANL
ARNDT
HOSHI
BASQ
800 MeV
C_LL
Θ_CM
ANL
ARNDT
HOSHI
BASQ
800 MeV
C_SL
Θ_CM
ANL
ARNDT
HOSHI
BASQ

Figure 2

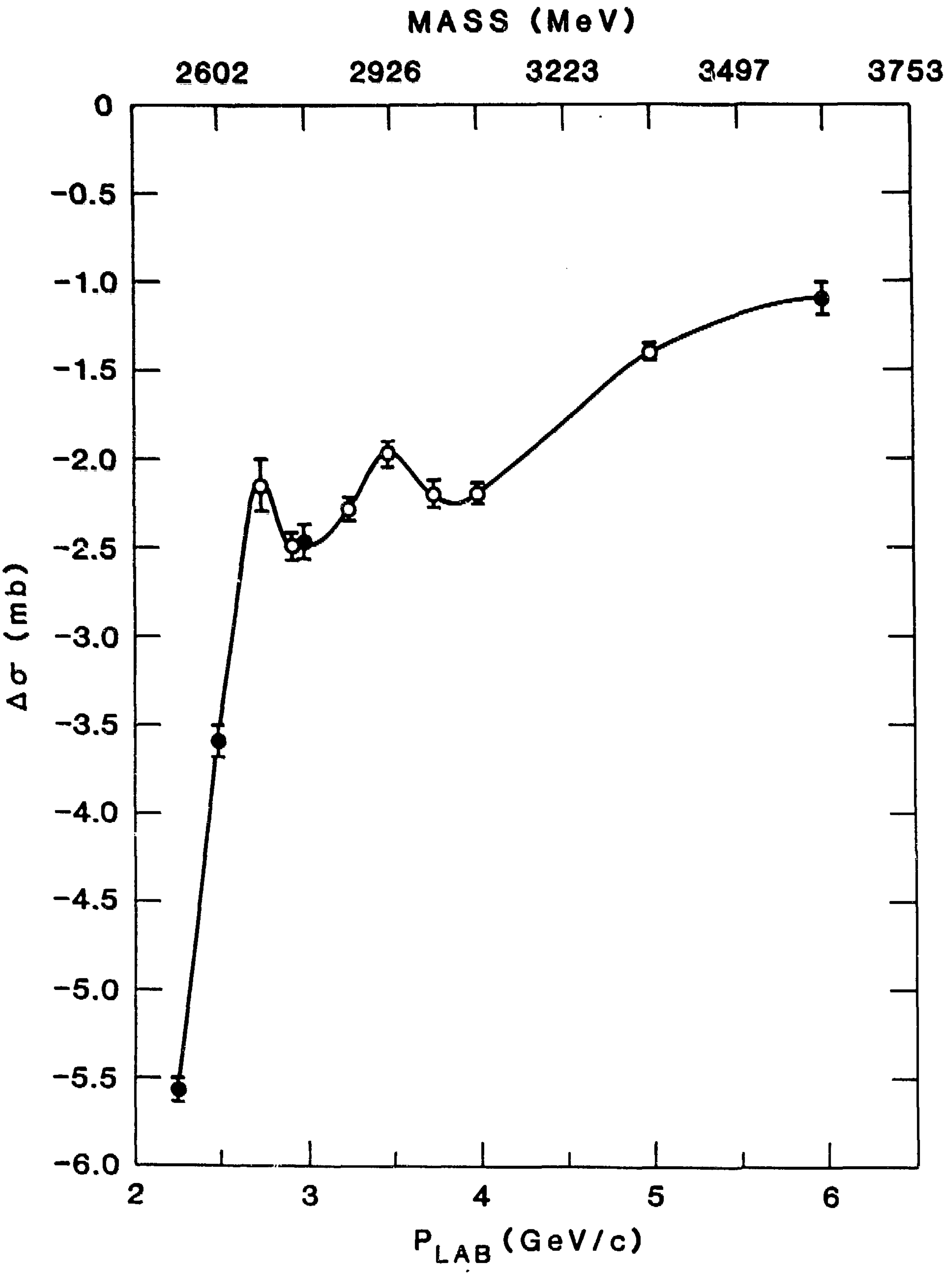
MASS (MeV)
2602
2926
3223
3497
3753
0
-0.5
-1.0
-1.5
-2.0
-2.5
-3.0
-3.5
-4.0
-4.5
-5.0
-5.5
-6.0
Δσ (mb)
2
3
4
5
6
P_LAB (GeV/c)

Figure 3

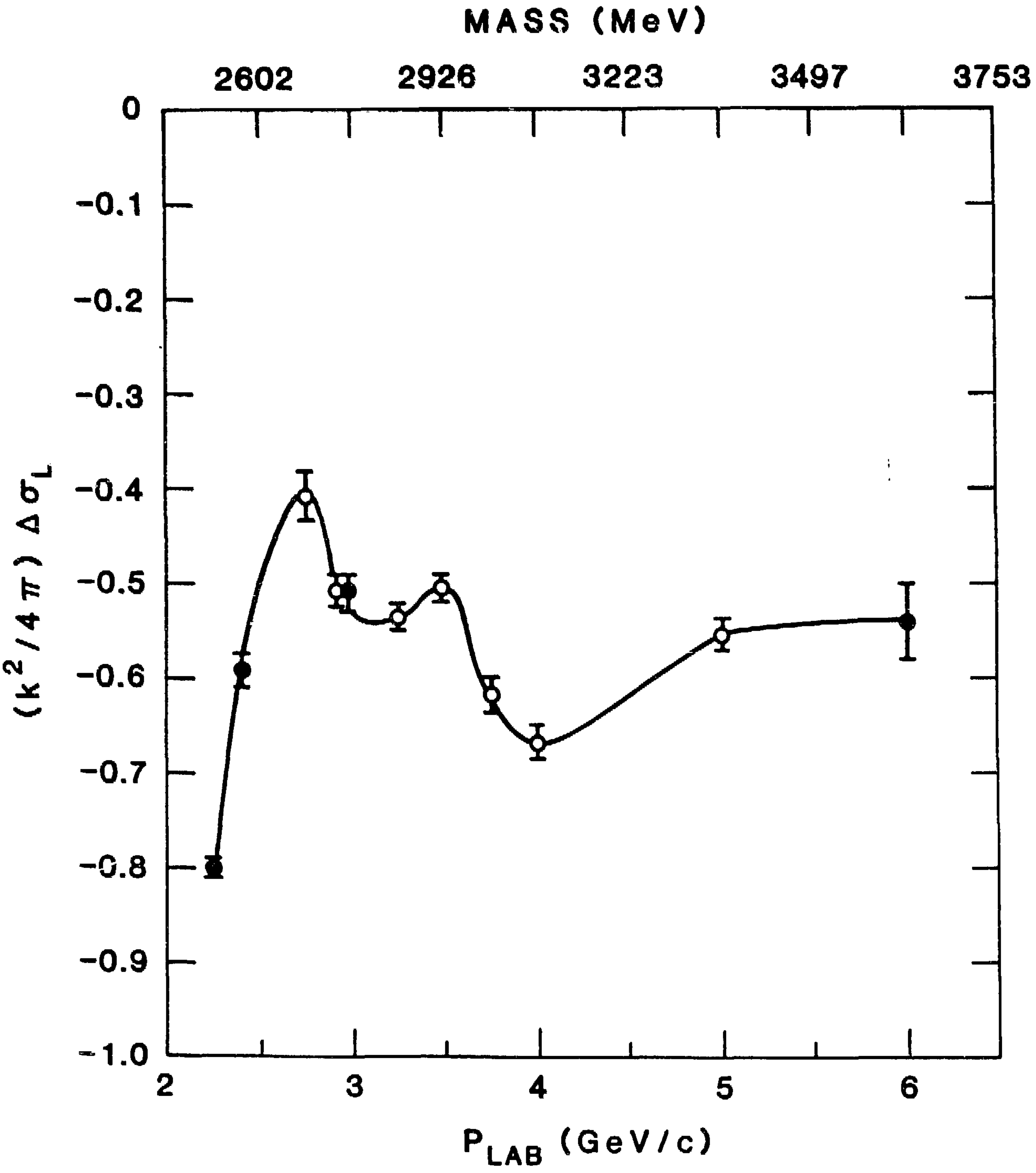
MASS (MeV)
2602
2926
3223
3497
3753
0
-0.1
-0.2
-0.3
-0.4
-0.5
-0.6
-0.7
-0.8
-0.9
-1.0
$(k^2/4\pi)\,\Delta\sigma_L$
2
3
4
5
6
P_{LAB} (GeV/c)

Figure 4